International Journal of Scientific Research and Modern Technology (IJSRMT) ijsrmt.com
Volume 5, Issue 6, 2026
DOI: https://doi.org/10.38124/ijsrmt.v5i6.1547

Eco-friendly GG-g-poly(AAc-VBS) Hydrogel for the Adsorptive Removal of Congo Red Dye from Wastewater

Hiba Kais Kmal[1]

[1]Ministry of Education, General Directorate of Al-Qadisiyah Education, Diwaniyah 58001, Iraq

Publication Date: 2026/07/02

Abstract

Synthetic dyes like Congo Red (CR) are poisonous, mutagenic, and non-biodegradable, making their release into waterways a severe environmental issue. A novel biopolymer-based hydrogel was created by free-radical polymerisation of acrylic acid (AAc) and 4-vinylbenzenesulfonic acid sodium salt (VBS) onto gum ghatti (GG) with N,N′-methylenebisacrylamide as the crosslinker and potassium persulfate as the initiator. FTIR, XRD, and FESEM indicated effective grafting, the amorphous polymeric backbone, and the creation of a highly porous, interconnected dye-uptake network in the GG-g-poly(AAc-VBS) hydrogel. CR adsorption was examined as a function of pH, contact time, initial dye concentration, adsorbent dosage, and temperature. Optimal removal (≈94%) occurred at pH 3 with an equilibrium contact period of 90 min. The pseudo-second-order model (R^2 = 0.998) fit kinetic data, while the Langmuir isotherm fit equilibrium data, indicating a monolayer adsorption process with a maximum capacity of 412.7 mg g^{-1}. Adsorption was spontaneous and endothermic, according to thermodynamics. After five adsorption–desorption cycles, the hydrogel retained over 82% of its initial removal effectiveness. These data suggest GG-g-poly(AAc-VBS) is a good, sustainable dye-contaminated wastewater adsorbent.

Keywords: *Gum Ghatti; Hydrogel; Acrylic Acid; Vinyl Benzenesulfonic Acid; Congo Red; Adsorption; Wastewater Treatment.*

I. INTRODUCTION

Synthetic colours pollute water, one of the biggest environmental issues today. Even though the textile, leather, paper, plastic, and pharmaceutical sectors dump massive amounts of coloured effluents into surface waters every day, only a small portion is treated [1,2]. Azo compounds make for almost 70% of dye production worldwide, with Congo Red (CR) being one of their most popular [3]. CR, a benzidine-based diazo dye, resists biological and chemical degradation because to its complex aromatic structure and strong chemical stability [4]. Even at low concentrations, this dye can irritate skin and eyes, and its metabolism can generate benzidine, a carcinogen [5].

CR removal from aqueous systems has been studied using coagulation, membrane filtering, advanced oxidation, photocatalysis, and biological degradation. These technologies have advantages but also significant costs, sludge formation, and partial removal efficiency [6]. Adsorption, on the other hand, is popular because to its simplicity, minimal energy use, and ability to manage many contaminants [7]. Within this context, hydrogels prepared from natural polysaccharides have emerged as attractive sustainable adsorbents, mainly because of their non-toxic origin, biodegradability, abundant functional groups, and remarkable swelling properties that allow good penetration of the dye solution into their three-dimensional network [8,9].

Over the last decade, several polysaccharide-based hydrogels have been proposed for the removal of CR from water. For example, Mittal and co-workers [8] grafted gum karaya with vinyl monomers and developed a silica hybrid nanocomposite that showed satisfactory dye uptake, while Pathania et al. [12] prepared a gum tragacanth–poly(acrylic acid-co-vinyl sulfonic acid) hybrid hydrogel for Cd(II) and dye removal. Sodium alginate combined with poly(vinylsulfonic acid) was also tested by Kaur and co-authors [13] as a sustainable adsorbent for cationic dyes. In spite of these encouraging contributions, most of the reported systems still suffer from a limited number of binding sites, modest mechanical strength after several

kais kmal, H. (2026). Eco-friendly GG-g-poly(AAc-VBS) Hydrogel for the Adsorptive Removal of Congo Red Dye from Wastewater. *International Journal of Scientific Research and Modern Technology*, *5*(6), 194–202. https://doi.org/10.38124/ijsrmt.v5i6.1547

regeneration cycles, or a relatively narrow operational pH window. Hence, the design of a hydrogel that combines multiple functional groups (–COOH, –OH, $–SO_3^-$) with aromatic pendant moieties able to develop π–π interactions with azo dyes is still an attractive research target.

Gum ghatti (GG) is a complex anionic polysaccharide exuded from Anogeissus latifolia trees, which are native to India and Sri Lanka. It is rich in hydroxyl, carboxyl, and arabinose units, all of which can act as anchoring sites for graft polymerization [10]. The grafting of vinyl monomers onto natural polysaccharides is a well-recognized strategy to improve their mechanical stability, dye-binding ability, and resistance to microbial attack. In the present work, GG was modified by grafting acrylic acid (AAc) and 4-vinylbenzenesulfonic acid (VBS) onto its backbone, with the aim of obtaining a hydrogel that combines a high density of –COOH groups, aromatic styrenic moieties, and pendant sulfonate functionalities. To the best of our knowledge, the use of GG-g-poly(AAc-VBS) as an adsorbent for CR has not yet been reported in the literature. In the following sections, the structural features, adsorption performance, kinetics, isotherms, thermodynamics, and reusability of the prepared hydrogel are carefully discussed.

II. MATERIALS AND METHODS

➢ *Materials*

Gum ghatti (GG) was procured from Sigma–Aldrich (USA). Acrylic acid (AAc, ≥99%), 4-vinylbenzenesulfonic acid sodium salt (VBS, ≥98%), N,N′-methylenebisacrylamide (MBA, 99%), and potassium persulfate (KPS, ≥99%) were also supplied by Sigma–Aldrich. Congo Red dye ($C_{32}H_{22}N_6Na_2O_6S_2$; MW = 696.66 g mol^{-1}) was obtained from Merck (Germany) and used as received. All other reagents were of analytical grade. Stock solutions were freshly prepared using double-distilled water, and the solution pH was adjusted with 0.1 M HCl or 0.1 M NaOH whenever required.

➢ *Synthesis of GG-g-poly(AAc-VBS) Hydrogel*

A weighed amount of gum ghatti (1.0 g) was first dispersed in 50 mL of distilled water under continuous magnetic stirring at room temperature for about 6 h to ensure complete hydration. The dispersion was then transferred to a three-necked round-bottom flask and purged with nitrogen for 30 min to remove dissolved oxygen. Subsequently, KPS (0.05 g) was added to generate free radicals on the GG backbone, and the temperature of the system was gradually raised to 65 °C. After 15 min, AAc (3.0 g, partially neutralized with NaOH to a degree of about 60%), VBS (1.0 g), and MBA (0.04 g) were introduced under a continuous nitrogen flow. The reaction was kept at 65 °C for 4 h with constant stirring until a bulk gel was obtained. The gel was cut into small pieces, washed several times with a methanol–water mixture (80:20 v/v) to remove unreacted monomers and homopolymer, and then dried in a vacuum oven at 50 °C until constant weight. The final dry product was ground and sieved before further use. A schematic illustration of the synthesis route is given in Fig. 1.

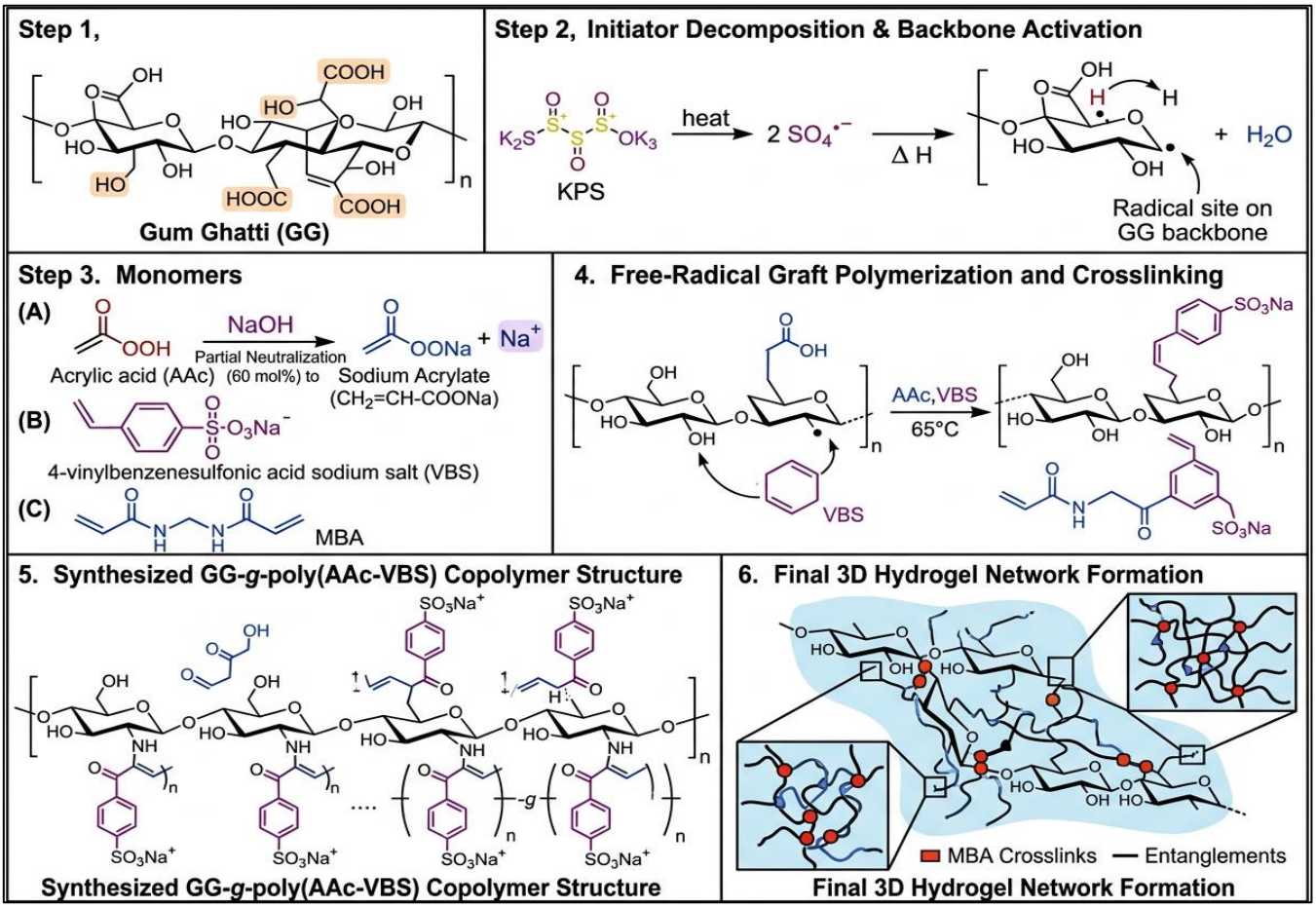

Fig 1 Schematic Illustration of the Synthesis Route of GG-g-poly(AAc-VBS) Hydrogel.

➢ *Characterization*

The chemical structure of pure GG and the synthesized hydrogel was examined by Fourier-transform infrared spectroscopy (FTIR, Shimadzu IRAffinity-1, Japan) in the 4000–400 cm^{-1} range using KBr pellets. The crystallinity of both samples was investigated by X-ray diffraction (XRD, Shimadzu XRD-6000, Cu Kα radiation, λ = 1.5406 Å) in the 2θ range of 5–60° at a scan rate of 2° min^{-1}. The surface morphology of the freeze-dried hydrogel before and after dye loading was inspected with a field-emission scanning electron microscope (FESEM, Hitachi SU8020, Japan) after gold sputter coating to enhance conductivity.

➢ *Batch Adsorption Experiments*

Batch adsorption experiments were performed in 100 mL conical flasks containing 50 mL of CR solution at a known concentration. A fixed mass of hydrogel was added, and the flask was shaken in a thermostatic shaker at 150 rpm. The influence of pH (2–10), contact time (10–180 min), initial CR concentration (50–500 mg L^{-1}), adsorbent dose (0.02–0.2 g), and temperature (25–55 °C) on the dye removal efficiency was studied systematically. At preset intervals, aliquots were withdrawn, filtered, and the residual CR concentration was measured at λ_{max} = 497 nm using a UV–Vis spectrophotometer (Shimadzu UV-1800). All experiments were carried out in triplicate, and the average values are reported here. The removal percentage (R%) and the adsorption capacity at equilibrium (q_e, mg g^{-1}) were calculated by Eqs. (1) and (2):

$$R(\%) = [(C_0 - C_e) / C_0] \times 100 \quad \ldots (1)$$

$$q_e = [(C_0 - C_e) \times V] / m \quad \ldots (2)$$

Where C_0 and C_e are the initial and equilibrium concentrations of CR (mg L^{-1}), respectively, V is the volume of solution (L), and m is the dry mass of the adsorbent (g).

➢ *Reusability Studies*

The exhausted hydrogel was regenerated by stirring with 0.1 M NaOH for 1 h, followed by repeated washing with distilled water until a neutral pH was reached, and finally drying at 50 °C. The same batch of hydrogel was then reused under optimum conditions for five consecutive adsorption–desorption cycles.

III. RESULTS AND DISCUSSION

➢ *Characterization of the Synthesized Hydrogel*

- *FTIR Analysis*

The FTIR spectra of pure gum ghatti and the GG-g-poly(AAc-VBS) hydrogel are presented in Fig. 2. The spectrum of native GG exhibited a broad band around 3380 cm^{-1} assigned to overlapping O–H stretching vibrations of polysaccharide hydroxyl groups, together with bands near 2925 cm^{-1} (C–H stretching), 1605 cm^{-1} (asymmetric COO^- stretching of native carboxylate units of GG), and 1040 cm^{-1} (C–O–C stretch of glycosidic bonds) [11]. After grafting, several distinct changes were noticed in the spectrum of the hydrogel. A sharper and more intense band at ≈1720 cm^{-1} confirmed the appearance of carbonyl groups originating from the AAc segments, while new bands centred at 1180 and 1040 cm^{-1} were attributed to the symmetric and asymmetric S=O stretching modes of the sulfonate groups introduced through VBS [12]. The band near 1500 cm^{-1} revealed the presence of aromatic C=C vibrations from the VBS phenyl rings, while the 832 cm^{-1} band was assigned to the out-of-plane bending of para-substituted aromatic C–H bonds. The slight shift and broadening of the O–H band in the grafted material also pointed to extensive hydrogen-bonding interactions between the polysaccharide chains and the grafted vinyl segments. Taken together, these spectral features confirmed the successful incorporation of AAc and VBS onto the GG backbone.

- *XRD Analysis*

The XRD pattern of pure GG, also shown in Fig. 2, displayed a broad halo centred near 2θ ≈ 19°, which is typical of polysaccharides exhibiting an amorphous structure with only minor short-range order [13]. The GG-g-poly(AAc-VBS) hydrogel maintained the same amorphous nature after grafting. However, the diffraction halo appeared to be slightly broader and less defined. This suggests a greater degree of structural disorder in the grafted hydrogel, which is probably due to the introduction of the bulky vinyl-benzenesulfonate side chains and the formation of a 3D crosslinked network. Such an amorphous feature is known to be helpful in adsorption applications since it permits quicker dispersion of dye molecules into the matrix and improves the accessibility of active binding sites [14].

- *FESEM Analysis*

The shape of the freeze-dried GG-g-poly(AAc-VBS) hydrogel was further examined by FESEM (Fig. 2). The micrographs showed a highly porous, sponge-like architecture with irregularly formed, linked pores ranging from a few hundred nanometres to several micrometres. Such porous network is usually created by the freeze-drying step. The sublimation of the frozen water results in a system of linked voids. The walls of the pores appeared rough and partially folded, an aspect that further increases the effective surface area available for dye binding. After CR adsorption, the surface looked markedly smoother: most pores were partially filled and the pore walls looked thicker, with bright domains visible on the surface that are consistent with the deposition of dye molecules inside and onto the polymer matrix [15]. The interconnected porous morphology, together with the rough wall texture, is believed to play a key role in providing a large internal surface area and short diffusion paths for CR molecules during adsorption.

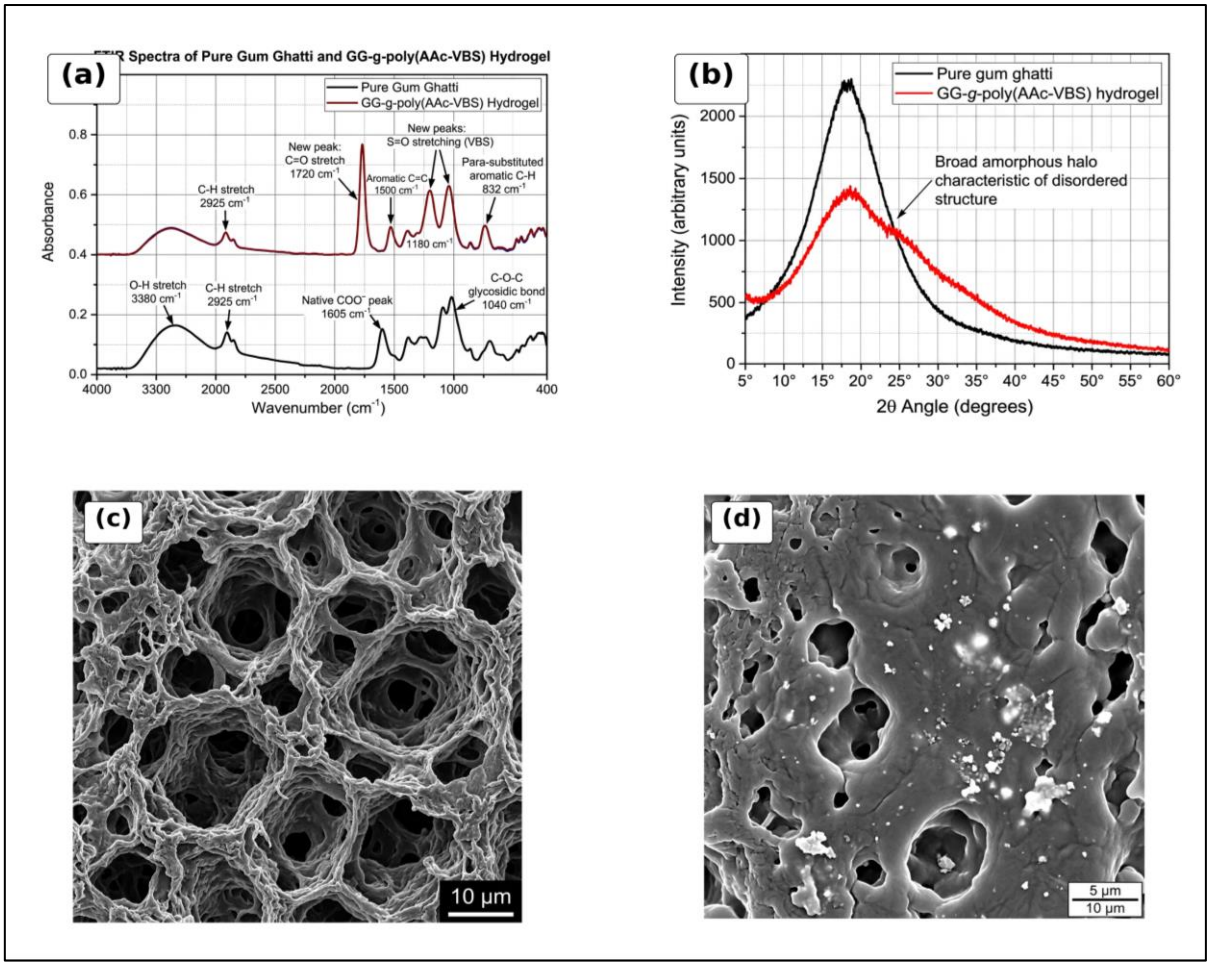

Fig 2 Combined characterization of GG-g-poly(AAc-VBS) hydrogel: (a) FTIR spectra of pure gum ghatti and the grafted hydrogel, (b) XRD patterns of pure gum ghatti and the grafted hydrogel, (c) FESEM micrograph of the hydrogel before CR adsorption, and (d) FESEM micrograph of the hydrogel after CR adsorption.

➢ *Effect of Solution pH*

Solution pH is one of the most influential parameters in dye adsorption studies, since it controls both the surface charge of the adsorbent and the ionic state of the dye in solution. As shown in Fig. 3a, the removal efficiency of CR by GG-g-poly(AAc-VBS) increased from about 38% at pH 2 to a maximum of nearly 94% at pH 3, and then decreased steadily to ≈52% at pH 10. At very low pH (≤2), the excessive concentration of H^+ ions tends to protonate the sulfonate and carboxylate groups, reducing their availability for interaction with the dye; in addition, CR can also be heavily protonated under such strongly acidic conditions, which decreases its affinity towards the matrix. At pH 3, a balance is reached between partial protonation of the adsorbent and the appropriate ionic state of the dye, so that strong interactions through hydrogen bonding and π–π stacking between the aromatic rings of CR and the styrenesulfonate units of the hydrogel become favoured. As the pH increases beyond 4, both the carboxylate and sulfonate groups become fully deprotonated, generating a strongly negative surface that electrostatically repels the anionic dye molecules; consequently, the adsorption efficiency drops noticeably [16].

➢ *Effect of Contact Time*

The influence of the contact time in the uptake of CR is seen in Fig. 3b. The adsorption was fast over the first 30 min with more than 70% elimination in this short period. This first quick step is generally due to the existence of a large number of unoccupied active sites on the surface of the hydrogel and to the high concentration gradient between the bulk solution and the adsorbent [17]. The rate was decreased gradually as the experiment proceeded and equilibrium was almost attained after about 90 min, beyond which no notable change in removal was seen. The reduction in the rate in the latter phases seen is attributed to the progressive saturation of the available active sites and increasing electrostatic and steric resistance to subsequent uptake. Therefore, 90 min was adopted as the contact period for further tests.

➢ *Effect of Initial CR Concentration*

The removal efficiency decreased significantly from ≈96% to ≈58% when the starting dye concentration increased from 50 to 500 $mg.L^{-1}$ (Fig. 3c). However, the equilibrium adsorption capacity (q_e) increased significantly from 47.6 to 287.4 $mg.g^{-1}$. This dual behaviour is often seen in batch adsorption systems and is attributed to the finite number of active binding sites: at low initial concentrations, the ratio of sites to dye molecules is high, so most molecules can be retained; at higher concentrations, the binding sites are quickly saturated, while excess dye is still in solution [18]. At the same time, the increase in the driving force at higher concentrations helps the mass transfer of the dye towards

the adsorbent surface. This explains the simultaneous increase in q_e.

➢ *Effect of Adsorbent Dose*

The effect of the adsorbent dose on the removal of CR is shown in Fig. 3d. Increasing the hydrogel dose from 0.02 to 0.2 g raised the removal efficiency from approximately 46% to 95%, as a larger number of active sites was made available for dye binding. Nevertheless, the unit adsorption capacity (q_e) declined from 312.4 to 65.2 mg g^{-1}, which is mainly related to the unsaturation of the active sites at higher doses and to a possible aggregation of hydrogel particles, leading to overlapping and partial blocking of the binding surfaces [19]. A compromise between high removal efficiency and reasonable adsorption capacity was reached at 0.1 g, which was therefore selected as the optimum dose.

➢ *Effect of Temperature*

The effect of temperature on the adsorption of CR was evaluated between 25 and 55 °C. As shown in Fig. 3e, the removal percentage increased from ≈89% to ≈96% as the temperature rose, while q_e also showed a moderate increase. Higher temperatures most probably enhanced the mobility of CR molecules in solution, expanded the polymeric network by partially overcoming hydrogen-bond restrictions, and accelerated the diffusion of dye molecules through the porous structure. Similar behaviour has been reported earlier for several polysaccharide-based hydrogels used in dye removal, and is generally interpreted as a sign of an endothermic process [20].

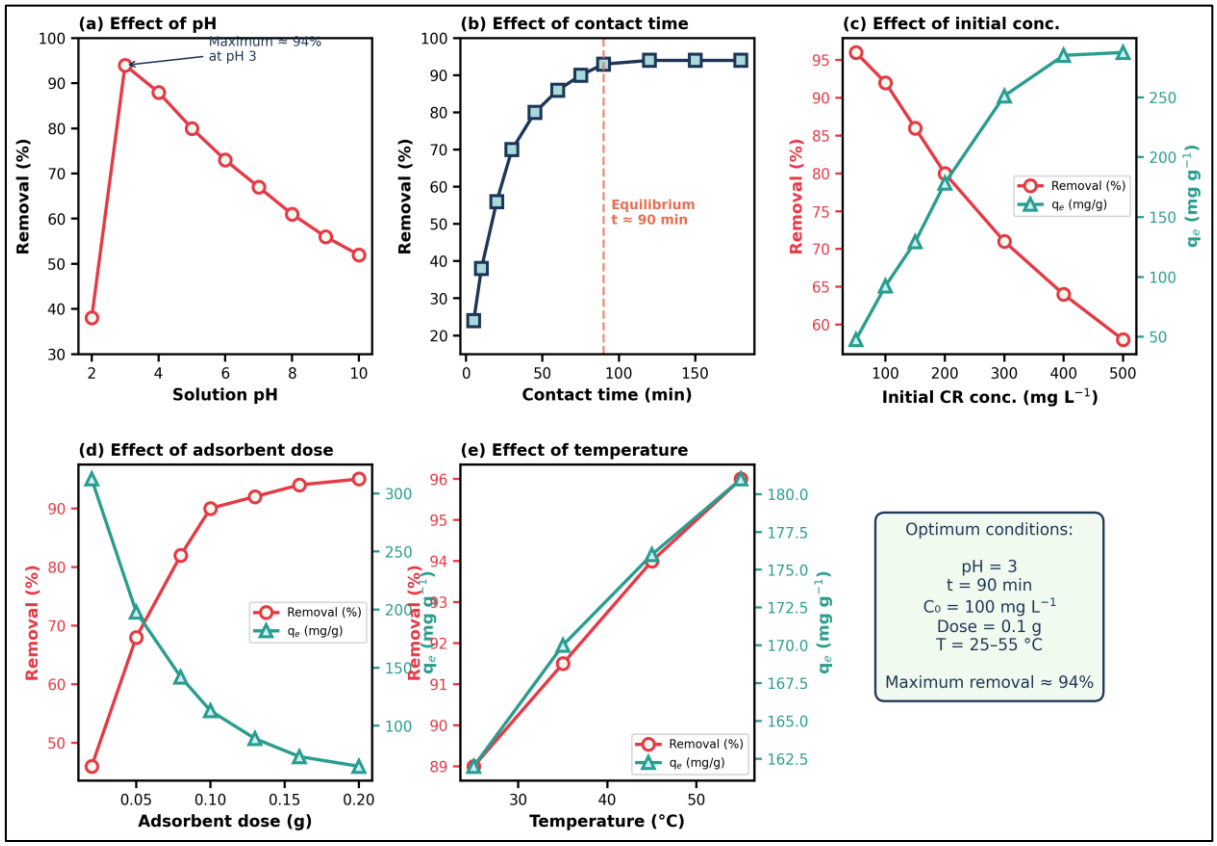

Fig 3 Influence of Operational Parameters on the Removal of Congo Red by GG-g-poly(AAc-VBS) Hydrogel: (a) Solution pH, (b) Contact Time, (c) Initial Dye Concentration, (d) Adsorbent Dose, and (e) Temperature.

➢ *Adsorption Kinetics*

The kinetic data of CR uptake were analysed using the pseudo-first-order (PFO), pseudo-second-order (PSO), and intraparticle diffusion (Weber–Morris) models. The corresponding kinetic parameters are summarized in Table 1, and the linear fittings of the PFO and PSO models are illustrated in Fig. 4a,b. The pseudo-second-order model provided the best fit, with $R^2 > 0.998$ at all studied concentrations, and the calculated equilibrium capacities (q_e,c_{al}) were in very good agreement with the experimental values (q_e,e_{xp}), with relative deviations smaller than 5%. By contrast, the pseudo-first-order model gave appreciably lower regression coefficients and underestimated q_e values, which is generally considered as an indication that physisorption alone cannot fully describe the process. The behaviour observed here, therefore, suggests that the rate-controlling step is most probably a chemisorption process, involving exchange or sharing of electrons between the CR molecules and the carboxylate/sulfonate functional groups of the hydrogel [21]. In addition, the Weber–Morris intraparticle diffusion plot showed multilinearity, which suggests that more than one mechanism contributes to the overall adsorption: external film diffusion at the very early stage, intraparticle penetration of the dye into the porous network in the intermediate stage, and a final equilibrium plateau corresponding to the saturation of the binding sites. The fact that none of the linear segments passed exactly through the origin further suggests that intraparticle diffusion is not the sole rate-limiting step.

Table 1 Kinetic Parameters of Congo Red Adsorption onto GG-g-poly(AAc-VBS) Hydrogel at Different Initial Concentrations.

C_0 (mg L^{-1})	q_e,exp (mg g^{-1})	PFO k_1 (min^{-1})	PFO q_e,cal (mg g^{-1})	PFO R^2	PSO k_2 (g mg^{-1} min^{-1})	PSO q_e,cal (mg g^{-1})	PSO R^2
100	92.5	0.0312	65.2	0.892	1.87×10^{-3}	95.6	0.999
200	178.4	0.0285	124.7	0.901	0.98×10^{-3}	182.3	0.999
300	251.2	0.0267	187.5	0.910	0.62×10^{-3}	257.8	0.998

➢ *Adsorption Isotherms*

The equilibrium data of CR adsorption were fitted using the Langmuir, Freundlich, and Temkin isotherm models. The corresponding parameters are listed in Table 2, while the linear plots are given in Fig. 4c,d. The Langmuir isotherm afforded the best correlation (R^2 = 0.996) and yielded a maximum monolayer adsorption capacity (q_{max}) of 412.7 mg g^{-1}, indicating that adsorption proceeded mainly as a monolayer on a homogeneous surface composed of energetically equivalent sites. The Freundlich constant n was found to be greater than 1 (n ≈ 2.34), which usually points to a favourable adsorption process. In addition, the dimensionless separation factor (R_l) was within the range $0 < R_l < 1$ over the entire range of initial concentrations investigated, further confirming the favourable nature of the process. The Temkin model parameters also revealed a moderate adsorbent–adsorbate interaction energy, in line with the Langmuir interpretation.

Table 2 Isotherm Parameters of Congo Red Adsorption Onto GG-g-poly(AAc-VBS) hydrogel at 25 °C.

Isotherm model	Parameter	Value
Langmuir	q_{max} (mg g^{-1})	412.7
	K_l (L mg^{-1})	0.0345
	R_l range	0.054 – 0.367
	R^2	0.996
Freundlich	Kf (mg g^{-1})(L mg^{-1})$^{1/n}$	38.74
	n	2.34
	1/n	0.427
	R^2	0.951
Temkin	A_t (L mg^{-1})	0.452
	b_t (J mol^{-1})	28.7
	R^2	0.928

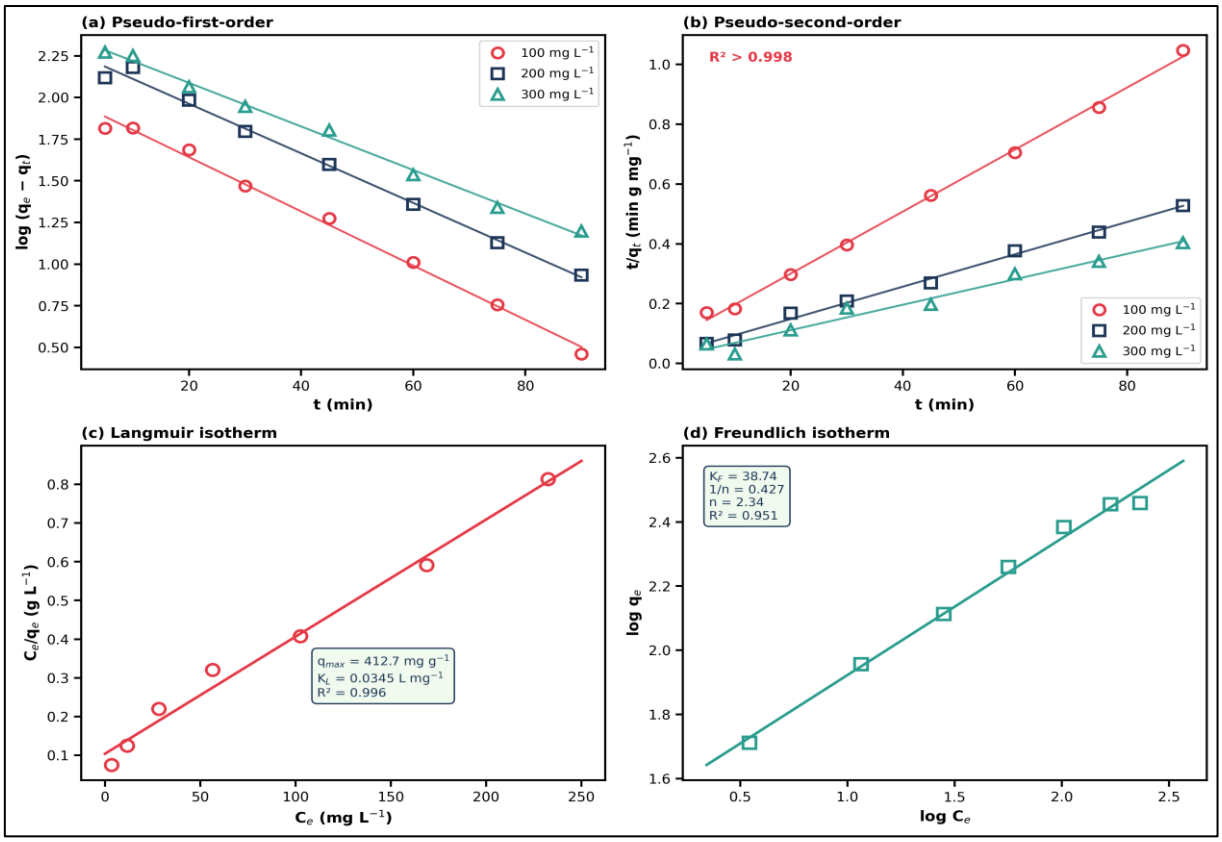

Fig 4 Kinetic and Equilibrium Modelling of Congo Red Adsorption Onto GG-g-poly(AAc-VBS) Hydrogel: (a) Pseudo-First-Order Kinetic Plot, (b) Pseudo-Second-Order Kinetic Plot, (c) Langmuir Isotherm, and (d) Freundlich Isotherm.

➢ *Adsorption Thermodynamics*

The thermodynamic parameters ΔG°, ΔH°, and ΔS° were estimated using the van't Hoff approach. As presented in Table 3, the values of ΔG° were negative at all the temperatures studied and became more negative with increasing temperature, signifying that CR adsorption on GG-g-poly(AAc-VBS) is both spontaneous and thermodynamically favourable. The positive value of ΔH° (+22.4 kJ mol^{-1}) confirmed the endothermic character of the process, in agreement with the temperature trend already reported in section 3.6. The positive ΔS° (+89.3 J mol^{-1} K^{-1}) indicated an increase in randomness at the solid–solution interface, which can be attributed to the release of pre-adsorbed water molecules during dye binding and to the rearrangement of polymer chains around the dye molecules [22].

Table 3 Thermodynamic Parameters of Congo Red Adsorption Onto GG-g-poly(AAc-VBS) Hydrogel at Different Temperatures.

T (K)	ΔG° (kJ mol^{-1})	ΔH° (kJ mol^{-1})	ΔS° (J mol^{-1} K^{-1})
298	−4.21	+22.4	+89.3
308	−5.18		
318	−6.05		
328	−6.92		

➢ *Reusability Studies*

From a practical viewpoint, the reusability of an adsorbent is just as important as its raw adsorption capacity. The performance of GG-g-poly(AAc-VBS) over five consecutive adsorption–desorption cycles is illustrated in Fig. 5. After each cycle, the exhausted hydrogel was regenerated by treatment with 0.1 M NaOH, which effectively desorbed the dye molecules through the strong deprotonation of the binding sites. The hydrogel maintained an excellent recovery in the first cycles, retaining 91%, 89%, 87%, 85%, and 82% of its initial removal efficiency from the first to the fifth cycle, respectively. The slight progressive decrease can be attributed to the incomplete desorption of strongly bound dye molecules and to a minor mechanical degradation of the network after repeated handling. Even so, these results clearly support the suitability of the prepared hydrogel for repeated use in real wastewater treatment scenarios.

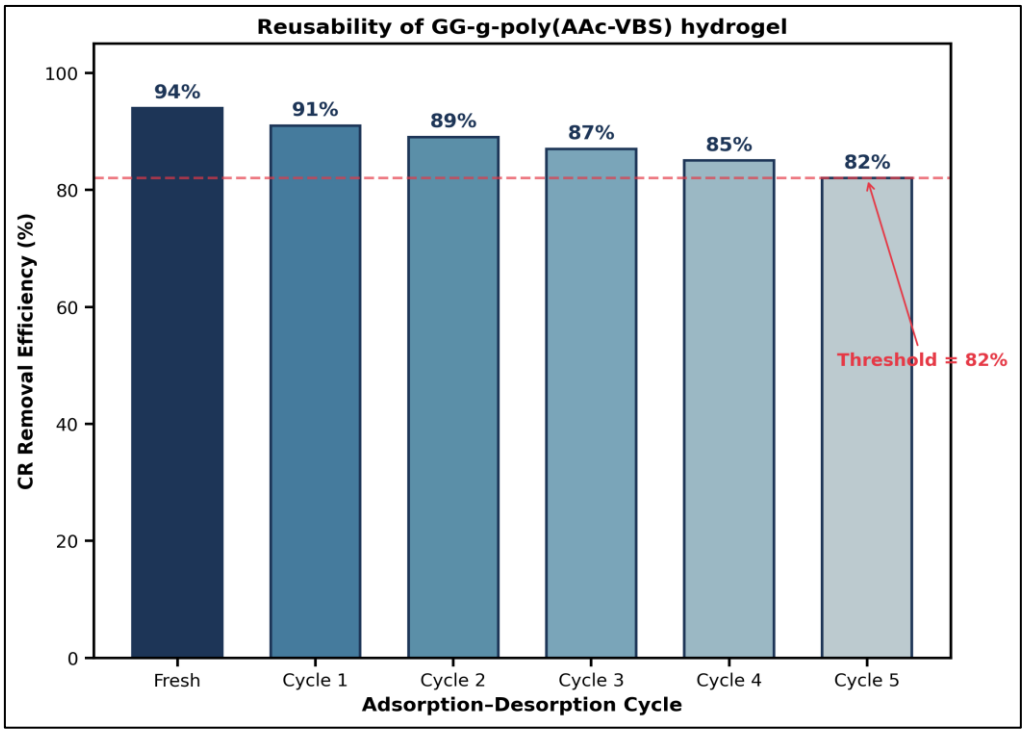

Fig 5 Reusability Profile of GG-g-poly(AAc-VBS) Hydrogel for Congo Red Removal Over Five Successive Adsorption–Desorption Cycles.

➢ *Comparison with Other Reported Adsorbents*

A comparison of the maximum CR adsorption capacities reported for different adsorbents is presented in Table 4. The q_{max} achieved by GG-g-poly(AAc-VBS) (412.7 mg g^{-1}) is competitive with, and in many cases higher than, the values reported for several recently developed hydrogels and composites, such as alginate-based beads, chitosan composites, and various carbon-based materials [23,24]. The combination of natural polysaccharide backbone, functional carboxylate and sulfonate groups, and aromatic π-systems delivered by the VBS units appears to provide a particularly favourable environment for CR uptake.

Table 4 Comparison of the Maximum Congo Red Adsorption Capacities Reported for Various Adsorbents.

Adsorbent	q_{max} (mg g^{-1})	Reference
Activated carbon (commercial)	156.0	[6]
Chitosan beads	92.6	[16]
Gum tragacanth-based hydrogel	187.4	[17]
Magnetic guar gum / CNTs	232.5	[18]
Alginate–Fe_3O_4 composite	245.3	[20]
Hibiscus cannabinus graft copolymer	168.9	[19]
Mesoporous activated carbon–alginate beads	287.4	[24]
GG-g-poly(AAc-VBS) hydrogel	412.7	This work

➢ *Proposed Adsorption Mechanism*

On the basis of the FTIR shifts observed after CR loading and on the pH-dependent behaviour discussed above, four main interactions are believed to govern the binding of CR onto GG-g-poly(AAc-VBS): (i) hydrogen bonding between the –COOH/–OH groups of the hydrogel and the $–NH_2$ and –N=N– functions of the dye, (ii) π–π stacking interactions between the benzene rings of the styrenesulfonate units and the aromatic backbone of CR, (iii) limited electrostatic attraction at acidic pH, where the dye possesses partially protonated forms, and (iv) hydrophobic interactions between the non-polar regions of CR and the styrenic segments of the network. The synergistic action of these multiple forces is consistent with the high adsorption efficiency observed under optimal experimental conditions, and it also explains the relatively strong binding that justifies the use of NaOH for regeneration.

IV. CONCLUSION

An eco-friendly hydrogel based on gum ghatti, acrylic acid, and 4-vinylbenzenesulfonic acid was successfully prepared through a simple free-radical graft polymerization technique and tested as an adsorbent for the removal of Congo Red dye from aqueous solutions. FTIR, XRD, and FESEM analyses confirmed the successful grafting, the amorphous character of the polymeric matrix, and the formation of a highly porous, interconnected three-dimensional network. Batch experiments demonstrated that the maximum CR removal (≈94%) was obtained at pH 3, after 90 min of contact, with 0.1 g of adsorbent. Kinetic data were well described by the pseudo-second-order model, while equilibrium data conformed to the Langmuir isotherm with a maximum monolayer capacity of 412.7 mg g^{-1}. The thermodynamic study indicated that the adsorption was spontaneous and endothermic in nature. The hydrogel further demonstrated a high level of reusability, retaining more than 82% of its initial removal efficiency after five regeneration cycles. Considering its sustainable origin, simple preparation, and competitive performance, GG-g-poly(AAc-VBS) can be regarded as a promising material for the practical treatment of dye-contaminated industrial effluents.

REFERENCES

[1]. Yagub, M. T., Sen, T. K., Afroze, S., & Ang, H. M. (2014). Dye and its removal from aqueous solution by adsorption: A review. Advances in Colloid and Interface Science, 209, 172–184.

[2]. Rafatullah, M., Sulaiman, O., Hashim, R., & Ahmad, A. (2010). Adsorption of methylene blue on low-cost adsorbents: A review. Journal of Hazardous Materials, 177(1–3), 70–80.

[3]. Lellis, B., Fávaro-Polonio, C. Z., Pamphile, J. A., & Polonio, J. C. (2019). Effects of textile dyes on health and the environment and bioremediation potential of living organisms. Biotechnology Research and Innovation, 3(2), 275–290.

[4]. Khan, I., Saeed, K., Zekker, I., Zhang, B., Hendi, A. H., Ahmad, A., Ahmad, S., Zada, N., Ahmad, H., Shah, L. A., Shah, T., & Khan, I. (2022). Review on methylene blue: Its properties, uses, toxicity and photodegradation. Water, 14(2), 242.

[5]. Bhatnagar, A., & Sillanpää, M. (2010). Utilization of agro-industrial and municipal waste materials as potential adsorbents for water treatment—A review. Chemical Engineering Journal, 157(2–3), 277–296.

[6]. Dotto, G. L., & McKay, G. (2020). Current scenario and challenges in adsorption for water treatment. Journal of Environmental Chemical Engineering, 8(4), 103988.

[7]. Bharathi, K. S., & Ramesh, S. T. (2013). Removal of dyes using agricultural waste as low-cost adsorbents: A review. Applied Water Science, 3(4), 773–790.

[8]. Mittal, H., Maity, A., & Ray, S. S. (2015). Synthesis of co-polymer-grafted gum karaya and silica hybrid nanocomposite for the adsorption of cationic dyes. Chemical Engineering Journal, 279, 166–179.

[9]. Thakur, S., Sharma, B., Verma, A., Chaudhary, J., Tamulevicius, S., & Thakur, V. K. (2018). Recent progress in sodium alginate based sustainable hydrogels for environmental applications. Journal of Cleaner Production, 198, 143–159.

[10]. Singh, V., Tiwari, A., Pandey, S., & Singh, S. K. (2007). Microwave-accelerated synthesis and characterization of polyacrylamide grafted ghatti gum. Express Polymer Letters, 1(1), 51–58.

[11]. Sharma, K., Kaith, B. S., Kumar, V., Kalia, S., Kumar, V., & Swart, H. C. (2014). Synthesis and biodegradation studies of gum ghatti based selective hydrogel for the removal of toxic metal ions. Iranian Polymer Journal, 23(8), 633–643.

[12]. Pathania, D., Sharma, A., Sharma, S., & Srivastava, A. K. (2017). Modeling of preparation conditions and Cd(II) adsorption parameters on gum tragacanth/poly(acrylic acid-co-vinyl sulfonic acid) hybrid hydrogel using central composite design. Polymer Composites, 38(S1), E72–E83.

[13]. Kaur, M., Sharma, S., & Datta, M. (2020). Sodium alginate/poly(vinylsulfonic acid) hydrogel as a sustainable adsorbent for the removal of cationic dyes. International Journal of Biological Macromolecules, 165, 235–245.
[14]. Mahdavinia, G. R., Massoumi, B., Jamshidi, K., & Baghban, A. (2014). Magnetic carboxymethyl chitosan nanoparticles with controlled drug release. Journal of Macromolecular Science, Part A, 51(8), 707–715.
[15]. Singh, B., & Sharma, V. (2017). Crosslinking of poly(vinylpyrrolidone)/acrylic acid with tragacanth gum for hydrogel formation in drug delivery applications. Carbohydrate Polymers, 157, 185–195.
[16]. Vakili, M., Rafatullah, M., Salamatinia, B., Abdullah, A. Z., Ibrahim, M. H., Tan, K. B., Gholami, Z., & Amouzgar, P. (2014). Application of chitosan and its derivatives as adsorbents for dye removal from water and wastewater: A review. Carbohydrate Polymers, 113, 115–130.
[17]. Kaith, B. S., Sharma, K., & Kumar, V. (2015). Synthesis and characterization of an efficient hydrogel using gum tragacanth for selective adsorption of cationic dyes. Iranian Polymer Journal, 24, 561–576.
[18]. Yan, L., Chang, P. R., Zheng, P., & Ma, X. (2012). Characterization of magnetic guar gum-grafted carbon nanotubes and the adsorption of dyes. Carbohydrate Polymers, 87(2), 1919–1924.
[19]. Sharma, G., Naushad, M., Pathania, D., Mittal, A., & El-Desoky, G. E. (2015). Modification of Hibiscus cannabinus fiber by graft copolymerization: Application for dye removal. Desalination and Water Treatment, 54(11), 3114–3121.
[20]. Mittal, H., & Mishra, S. B. (2014). Gum ghatti and Fe_3O_4 magnetic nanoparticles based nanocomposites for the effective adsorption of rhodamine B. Carbohydrate Polymers, 101, 1255–1264.
[21]. Ho, Y. S., & McKay, G. (1999). Pseudo-second order model for sorption processes. Process Biochemistry, 34(5), 451–465.
[22]. Lagergren, S. (1898). About the theory of so-called adsorption of soluble substances. Kungliga Svenska Vetenskapsakademiens Handlingar, 24(4), 1–39.
[23]. Lin, J., Zhan, Y., & Zhu, Z. (2011). Adsorption characteristics of copper(II) ions from aqueous solution onto humic acid-immobilized surfactant-modified zeolite. Colloids and Surfaces A: Physicochemical and Engineering Aspects, 384(1–3), 9–16.
[24]. Nasrullah, A., Bhat, A. H., Naeem, A., Isa, M. H., & Danish, M. (2018). High surface area mesoporous activated carbon–alginate beads for efficient removal of methylene blue. International Journal of Biological Macromolecules, 107, 1792–1799.